International Journal of Nanoscience
Vol. 4, No. 1 (2005) 107–118

World Scientific
www.worldscientific.com

HAMILTONIAN LOGIC GATES: COMPUTING INSIDE A MOLECULE

C. JOACHIM and I. DUCHEMIN
The Nanoscience Group, CEMES-CNRS, 29, Rue J. Marvig
BP 4347 31055 Toulouse Cedex, France

J. FIURÁŠEK and N. J. CERF
Quantum Information and Communication, Ecole Polytechnique, CP 165
Université Libre de Bruxelles, 1050 Bruxelles, Belgium

Received 19 May 2004
Revised 4 October 2004

Using an intramolecular single-electron transfer process, we show how computing inside a quantum system can be performed using the time evolution driven by the preparation of the system in a nonstationary state. The molecule Hamiltonian is separated in three parts: the input, calculation, and output parts. Two optimization procedures are described in order to design an efficient monoelectronics level structure for molecular logic gates. An XOR gate and a half-adder using six electronic quantum levels are presented in a prospect to integrate a full logic gate inside a single molecule without forcing the molecule to have the shape of an electrical circuit. We foresee the merger of molecular electronics with quantum computation at the nanoscale.

Keywords: Unimolecular electronics; quantum computers; intramolecular logic gates; intramolecular electron transfer.

1. Introduction

Progress in atomic scale technology[1,2] put forward the possibility to access quantum electronic behavior inside a single molecule with a precision better than 0.1 nm. Therefore, it becomes important to evaluate the quantum resources available in a single molecule for designing, for example, unimolecular machines able to perform a computation. In a seminal paper, R. P. Feynman had already suggested to use the internal time-dependant evolution of a single quantum system to design a quantum computer.[3] In his view, a quantum computer consists of assembling N two-level quantum systems called qubits. One unit of information is encoded by each qubit, and the N qubits are placed in interaction along the time evolution of the system depending on the computer program.

We describe here another design resulting in a decrease of the number of roles assigned to the state vector and in an increase of the role played by the Hamiltonian.

Instead of encoding the inputs into the state vector, they are encoded in a separate part of the Hamiltonian compared to the one that drives the computation. This is in contrast to the R. P. Feynman design where the state vector describing the quantum state assumes three different roles at the same time: it carries in the input data (the preparation of which requires some energy), drives the computation, and carries out the result of the computation at a given and well-chosen time.

Our quantum system does not have a qubit structure and the source and drain electronic levels play the role of a "driving qubit". They bring the necessary energy to drive the computation, preparing the full quantum system in a nonstationary state. As discussed in the following, this design have some advantages over a standard quantum computer design for integrating a whole logic gate inside a single molecule, hence to merge molecular electronics and quantum computers down to the nanoscale.[4]

In Sec. 2, the design of an Hamiltonian computer is provided with details on its possible hardware implementation. In Sec. 3, two different optimization strategies are proposed to design the calculation Hamiltonian as a function of the logic function to be achieved. In Sec. 4, two intramolecular XOR gates are devised, and a digital half-adder is presented in Sec. 5. The conclusion discusses steps toward the design of computing molecules.

2. Design Rules for an Hamiltonian Intramolecular Computer

In principle, computing within a single quantum system is a matter of controlling its quantum trajectory starting from a given nonstationary state.[5] In a pure spectroscopy version and with a single molecule electronically isolated from its surrounding during the computation, this initial preparation must populate the required excited states of the molecule with the good amplitudes and phases to encode the input data. During the time interval where the molecule can be considered as isolated, it will spontaneously evolve in time. The result of the computation is obtained performing a measurement of the population (in time or in average) of the output-dedicated quantum levels of the molecule. Aside from the design of the molecule, the endeavor here is to encode and decode the information, and to control the quantum trajectory of the molecule in its formal quantum state space.[5]

Before describing in detail the structure of our Hamiltonian, let us take a simple example of a molecule with four electronic levels active in the computation operation. This number of levels was chosen to keep a topological separation between the input and the output states of the logic gate. One example leading to an XOR logic gate behavior with such a four-level system is the Hamiltonian $h_{\mathrm{XOR}} = e(|1\rangle\langle 1| - |2\rangle\langle 2| + |3\rangle\langle 3| - |4\rangle\langle 4|)$. We construct four peculiar XOR nonstationary states on the $|i\rangle\langle i|$ basis with e the corresponding eigenvalues:

$$|\mathrm{I}_1\rangle = 0.5\,(-|1\rangle + |2\rangle + |3\rangle + |4\rangle)\,, \tag{1a}$$

$$|\mathrm{I}_2\rangle = 0.5\,(|1\rangle - |2\rangle + |3\rangle + |4\rangle)\,, \tag{1b}$$

Table 1. Truth table of a simple XOR four-level quantum system.

Logic input	λ_1	λ_2	Max. of $\lvert\langle O_1 \rvert \phi(t)\rangle\rvert^2$
0 0	0	0	0
0 1	0	π	1
1 0	π	0	1
1 1	π	π	0

$$|\mathrm{O}_1\rangle = 2^{-1/2}\,(|1\rangle + |2\rangle)\,, \tag{1c}$$

$$|\mathrm{O}_2\rangle = 2^{-1/2}\,(|3\rangle - |4\rangle)\,. \tag{1d}$$

The input states of this XOR are defined by preparing at $t = 0$ the above four-level system in the nonstationary states: $|\phi(0)\rangle = 2^{-1/2}\,(\mathrm{e}_1^{i\lambda_1}|\mathrm{I}_1\rangle + \mathrm{e}_2^{i\lambda_2}|\mathrm{I}_2\rangle)$, with λ_1 and λ_2 encoding the input bits as defined in Table 1. The logic output of the XOR gate is determined by measuring the occupation of the state $|\mathrm{O}_1\rangle$ (see Table 1).

This example illustrates how a good choice of the calculation Hamiltonian results in a quantum system behaving like a digital logic gate. A few of its design principles are not very compatible with a passage from a formal quantum system to a real molecule: (1) the spectroscopy precision required to encode the input or to decode the output are incompatible with the present and certainly the near future experiments on single atomic or molecular systems; (2) in order to reliably extract the outcome of the computation, a large number of equivalent quantum systems must be used simultaneously. This clearly does not go in the direction of an ultimate miniaturization of a computer. A difficulty of miniaturizing stems from the uncertainty inherent to quantum measurements. Reducing quantum fluctuations can be obtained either by increasing the number of identical quantum systems in action, or by measuring the same single quantum system a large number of times.

Our Hamiltonian computing scheme is based on this second approach. The total Hamiltonian consists of an input Hamiltonian H_{in}, an output Hamiltonian H_{out}, and a calculation Hamiltonian H_{cal} (see Fig. 1). Each input bit of the calculation is encoded on the strength of a well-identified coupling constant α_n of H_{in}. Here comes the important role of the "driving qubit" ($|a\rangle, |b\rangle$) in Fig. 1. The nonstationary source state $|a\rangle$ is coupled only to the internal states via H_{in}. Each coupling value α_n is supposed to be controlled, at the atomic scale, for example, by the rotation of a well-identified chemical group in the full molecular system. This rotation can be triggered by the tip apex of an STM.[6] Therefore, the role of the spontaneous quantum evolution from the source $|a\rangle$ to the drain $|b\rangle$ level is to populate the internal electronic levels as a function of the coupling strength. The quantum fluctuations average out when the electron transfer process from $|a\rangle$ to $|b\rangle$ has occurred many times. An interesting solution to generate those driving states is to prepare the system using a tunnel junction with $|a\rangle$ electronically interacting with the electronic state of one electrode and $|b\rangle$ with the ones of the other electrode of the junction.[4]

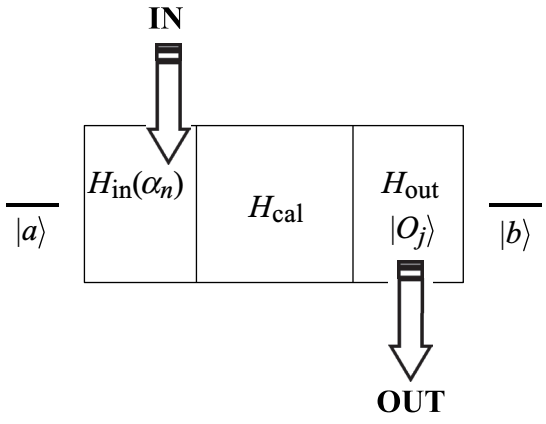

Fig. 1. Internal structure of the "driving qubit" ($|a\rangle$, $|b\rangle$) to realize an Hamiltonian logic gate. The input data are encoded in the α_n numbers that characterize the strength (or phase) of an electronic coupling inside the molecule. The outputs are determined by measuring the population of some output states supported by H_{out}.

Coupled to the drain level via the output Hamiltonian H_{out} in Fig. 1 and in order to read out the population of the output levels, a possibility is to include a rotating chemical group with a very low rotating barrier per output channel. Each chemical group would be in charge of averaging the number of electrons passing per second through this output level in route from the source to the drain level. Such rotating groups are acting like sub-nanometer scale intramolecular quantum thermometers. Their fluctuation amplitudes, detectable, for example, by near field techniques,[7] depend on the number of electrons per second exchanged between $|a\rangle$ and $|b\rangle$ through a specific output level.

Aside from the input H_{in} and output H_{out} Hamiltonians, the molecular Hamiltonian is completed by a central part H_{cal} in charge of controlling the quantum state trajectory from a given input configuration toward the good output states (Fig. 1). Here is the pure quantum time evolution part of our computer design driven by the preparation of the full system in the nonstationary state $|a\rangle$. Specific optimization tools have been developed to find an efficient H_{cal} as discussed in the next section.

3. Optimizing the Computing Part of the Hamiltonian

The optimization of H_{cal} depends on the strategy chosen to measure the result of the calculation. For example, the population of some output states $|\varphi_j\rangle$ belonging to the support of H_{out}, with j labeling the outcome of the calculation, can be measured at some specific time during the evolution. This optimization will be called "time optimization" in what follows. Alternatively, one can also choose to optimize only the maximum occupation of those states over time ("max optimization"). In both

cases, the occupation amplitude of the $|\varphi_j\rangle$ states given the input parameter α_n is

$$f_{j|n}(t) = \langle\varphi_j|\mathrm{e}^{-\mathrm{i}H(\alpha_n)t}|a\rangle \tag{2}$$

with $H(\alpha_n) = H_{\mathrm{in}}(\alpha_n) + H_{\mathrm{cal}} + H_{\mathrm{out}}$ being the Hamiltonian of the full system (Fig. 1), where the reference energy for the source $|a\rangle$ and drain $|b\rangle$ states is supposed to be zero.

In the "time optimization" approach, the measurement at a given fixed time t should discriminate between different subsets of output states that are generated from a common state $|a\rangle$ after time evolution governed by the P different Hamiltonians $H(\alpha_n)$. P is the total possible number of different input configurations on the computer. Each input generates a specific Hamiltonian $H(\alpha_n)$. Each $H(\alpha_n)$ is the generator of a time-dependent quantum evolution leading to the good output configuration for a given input configuration. In order to design the best Hamiltonian H_{cal} inside $H(\alpha_n)$, we have introduced the figure of merit:

$$F = 1/P \sum_{j,n} C_{j,n}|f_{j|n}(t)|^2\,, \tag{3}$$

where the constants $C_{j,n} \in \{0,1\}$ are suitably chosen so that F represents the probability of the correct outcome averaged over all P possible inputs. We thus look for the Hamiltonian H_{cal} that maximizes F at a fixed given time t for this "time optimization" approach.

The details of the optimization procedure are presented elsewhere.[8] We will only sketch the main steps here. With the help of first-order perturbation theory, one can calculate the variation δF of the fidelity F induced by a small variation δH_{cal} of the H_{cal} matrix elements. A properly chosen modification of H_{cal} using a specific complementary operator leading to a new version of the calculating part of the Hamiltonian: $H_{\mathrm{cal}} + \varepsilon\,\Sigma(X_j + X_j^+)$,[8] leads to $\delta F \geq 0$. This provides a variational iterative algorithm that finds the optimal H_{cal} by following a steepest ascent strategy. It should be noted that, by construction, this steepest ascent method can only yield a local maximum. Therefore, in order to obtain a fair estimate of the global maximum, the numerical optimization was repeated many times, starting with randomly chosen initial H_{cal}, and selecting after the best solution Hamiltonian.

In the "max optimization" approach, the outputs are encoded by the maximum absolute value of the $f_j(t)$ amplitudes reached over time. Here, our optimization criterion determines the H_{cal} matrix elements in such a way that the extremum of the $f_j(t)$ over time gives a logic output "1" or "0" depending on the values of the input parameters α_n. Starting from Eq. (2), the unitary matrix $U(\alpha_n)$ diagonalizing $H(\alpha_n)$ leads to the well-known decomposition

$$f_j(t) = \sum_k U_{jk}^{-1}(\alpha_n)\mathrm{e}^{-iEk(\alpha_n)t}U_{ka}(\alpha_n)\,. \tag{4}$$

This means that the extremum of each $f_j(t)$ over time is bounded by

$$|f_j(t)| < \sum_k |U_{jk}(\alpha_n)^{-1}| \quad |U_{ka}(\alpha_n)|\,. \tag{5}$$

Here, our "max optimization" criterion is as follows: for each input configuration, the $H_{\rm cal}$ matrix elements are optimized to lower or maximize Eq. (5) depending on the logic function that $H(\alpha_n)$ is supposed to realize. The target lower value chosen is always zero corresponding to the "0" logic state and the logic "1" corresponds always to a renormalized maximum amplitude depending on the number of $|\varphi_j\rangle$ which are supposed to be at the same time near their limit sup.

4. Examples of Hamiltonian XOR Gates

The two optimization procedures (time or max) described before were applied to the case of a simple XOR gate. Practical constrains about the preparation of system, the driving of the computation, and the output indicates that a minimum quantum system of six levels is well adapted for an XOR including the two quantum states required to drive the computation. For simplicity, a phase input may be chosen, as in the example of a four-level XOR gate discussed in Sec. 2. But for symmetry reason, such a phase input does not work for an AND gate. Therefore, we have chosen here to input the data on the strength of the coupling α_1 and α_2 between the source state $|a\rangle$ and the $H_{\rm cal}$ states $|1\rangle$ and $|2\rangle$, respectively, as presented in Fig. 2. The outputs are determined by measuring the population of state $|3\rangle$ after a few oscillations from $|a\rangle$ to $|b\rangle$ through the four intermediate levels coupled by $H_{\rm cal}$ (Fig. 2). Notice that these time-dependent oscillations can be characterized by their secular Rabi frequency[9] even if the $|b\rangle$ state is generally far from being reached

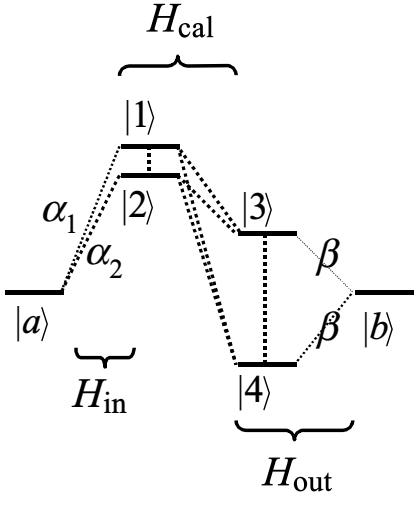

Fig. 2. Detailed level structure of the six-level XOR gate optimized with the "time" optimization procedure. The three parts of the Hamiltonian are indicated together with the source $|a\rangle$ and drain $|b\rangle$ states. The input is determined by the α_1 and α_2 coupling strengths according to the truth Table 1. The XOR output is obtained by measuring the population of state $|3\rangle$. The dashed lines indicate the electronically coupled states.

during a full oscillation period. In the case of "time optimization", an example of optimized XOR Hamiltonian H_{cal} reads in the basis $\{|1\rangle, |2\rangle, |3\rangle, |4\rangle\}$ as:

$$H_{\text{cal}} = \begin{pmatrix} 1.4607 & -3.2687 & 0.3011 & 3.7692 \\ -3.2687 & 1.2413 & 0.2816 & 3.9233 \\ 0.3011 & 0.2816 & 0.6331 & 1.9971 \\ 3.7692 & 3.9233 & 1.9971 & -0.7491 \end{pmatrix} \tag{6}$$

with $H_{\text{in}}(\alpha_n) = \alpha_1(|a\rangle\langle 1| + (|1\rangle\langle a|) + \alpha_2(|a\rangle\langle 2| + |2\rangle\langle a|), \alpha_i = 2\,\text{eV}$ for logic state "0" and $2/3\,\text{eV}$ for logic state "1", $H_{\text{out}} = \beta(|b\rangle\langle 3| + |3\rangle\langle b|) + \beta(|b\rangle\langle 4| + |4\rangle\langle b|)$ with $\beta = 0.5\,\text{eV}$. The coupling strengths were selected to be compatible with the values usually chosen in a topological Hückel molecular orbital approximation of a π molecular orbital structure of a conjugated molecule.

With the same level structure as the one presented in Fig. 2 for the "time" optimized XOR, the "max optimization" criterion (5) leads to the following optimized H_{cal} Hamiltonian:

$$H_{\text{cal}} = \begin{pmatrix} 0.1351 & 1.3508 & 0.7155 & 0.2393 \\ 1.3508 & 0.1346 & -0.7166 & -0.2376 \\ 0.7155 & -0.7166 & -0.5101 & 1.4760 \\ 0.2393 & -0.2376 & 1.4760 & 1.8169 \end{pmatrix} \tag{7}$$

with α_i and β defined as previously.

In both cases, the chosen $|\varphi_j\rangle$ output level is the electronic level $|3\rangle$. Notice that, like in any nonlinear optimization procedure, several locally optimal Hamiltonians can be found. A robustness study remains to be performed to ensure that those Hamiltonian logic gates are not too sensitive to a small deviation in the matrix elements of the H_{cal} Hamiltonian. This will be particularly important for the design of a molecule according to the six-level structure found by optimization.

The truth tables of the two optimization procedures are given in Tables 2 and 3. The best way to illustrate this optimization is to follow the $|\langle 3|\phi(t)\rangle|^2$ population in time, as presented in Fig. 3 where $|\phi(0)\rangle = |a\rangle$. Notice that $|a\rangle$ is the initial driving state of the six-level system. In both cases, the time evolution of the population is

Table 2. Truth table of an optimized XOR gate using the "time" optimization procedure leading to the H_{cal} Hamiltonian (6).

Logic input	α_1	α_2	$\lvert\langle 3\rvert\phi(t)\rangle\rvert^2$ at $t = 6.28$
0 0	2	2	2.53×10^{-3}
0 1	2	2/3	0.937
1 0	2/3	2	0.937
1 1	2/3	2/3	6.46×10^{-3}

Table 3. Truth table of an XOR gate using the "max" optimization procedure leading to the $H_{\rm cal}$ Hamiltonian (7).

Logic input	α_1	α_2	Max. of $\lvert\langle 3\lvert\phi(t)\rangle\rvert^2$
0 0	2	2	3.97×10^{-5}
0 1	2	2/3	0.98062
1 0	2/3	2	0.98062
1 1	2/3	2/3	2.106×10^{-5}

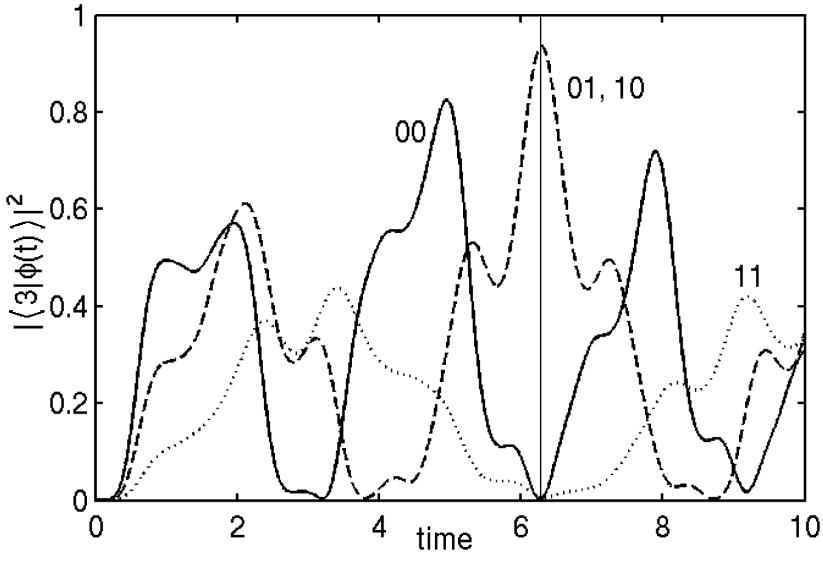

(a)

Fig. 3. Time evolution of the population of the output level $|3\rangle$ for the XOR gate obtained with a "time" (a) or "max" (b) optimization. For (a), the population is plotted for the four different logic inputs 00, 01, 10, and 11. The curves for inputs 01 and 10 are practically identical, so the population for input 01 is only shown. The readout time $t = 2\pi = 6.28$ is indicated by a vertical line. For (b) and according to Table 3, the 01 and 10 logic inputs lead to almost the same output population of state $|3\rangle$, while for the 00 and 11 inputs, this state $|3\rangle$ and state $|4\rangle$ are not reached at all. The corresponding $H_{\rm cal}$ are given in Eqs. (6) and (7), respectively (the time scale is $h/2e\pi$).

almost periodic. The "time" optimization leads to a clear difference in the occupation amplitude at the precise time of measurement ($t = 2\pi = 6.28$ in appropriate units), while the "max" optimization leads to a very clear difference between the "0" and the "1" logic level over time. The fidelity defined by Eq. (3) is almost 100% in both cases.

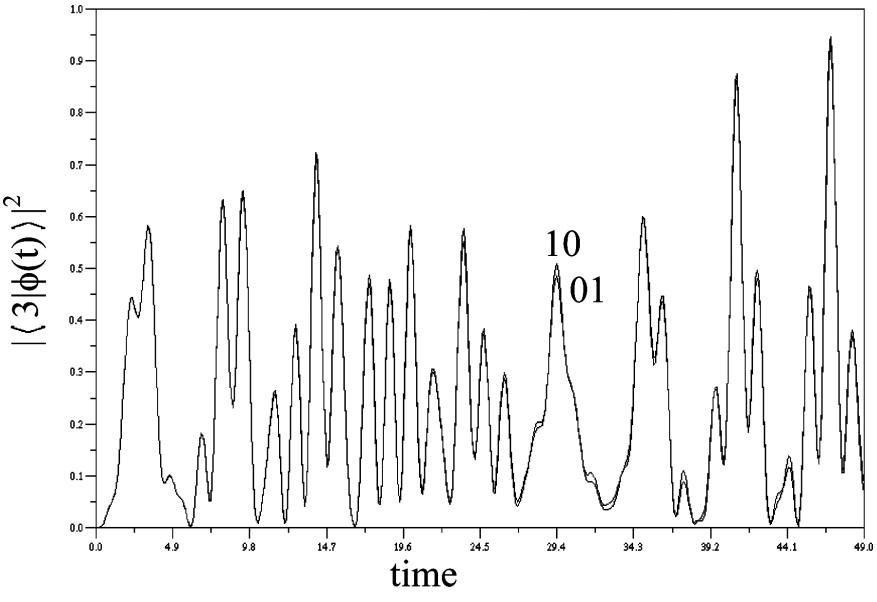

(b)

Fig. 3. (*Continued*)

5. Optimizing an Hamiltonian Half-Adder

In digital electronics, an half-adder is made out of an XOR gate in parallel with an AND gate using the same input data. With our Hamiltonian logic gate design, an AND gate can also be optimized with a six-level system following the optimization procedures described in Sec. 3. However, a simple quantum interconnection of this AND gate with the corresponding XOR gate does not permit to assemble an intramolecular H_{cal} sharing the same coupling strength inputs α_n. Instead of assembling a higher-dimensional system combining the two optimal H_{cal}, we have found that a well-optimized six-level system is enough to obtain an Hamiltonian half-adder. For example, in the case of a "max" optimization and for logic inputs encoded in the coupling strength as before, H_{cal} reads:

$$H_{\text{cal}} = \begin{pmatrix} 0.1613 & 0.0782 & -0.3582 & 0.1096 \\ 0.0782 & 0.1041 & 0.3288 & 0.0368 \\ -0.3582 & 0.3288 & -1.8420 & 0.1774 \\ 0.1096 & 0.0368 & 0.1774 & -0.5276 \end{pmatrix} \tag{8}$$

with α_n and β defined as previously. The truth table of this gate is presented in Table 4 while the time evolution of the $|\langle 3|\phi(t)\rangle|^2$ and $|\langle 4|\phi(t)\rangle|^2$ populations are presented in Fig. 4. Compared to the optimization of a logic gate with a single output, optimizing H_{cal} for two logic outputs leads to a large decrease of the maximum available population over time. This is due to the large amount of occupation

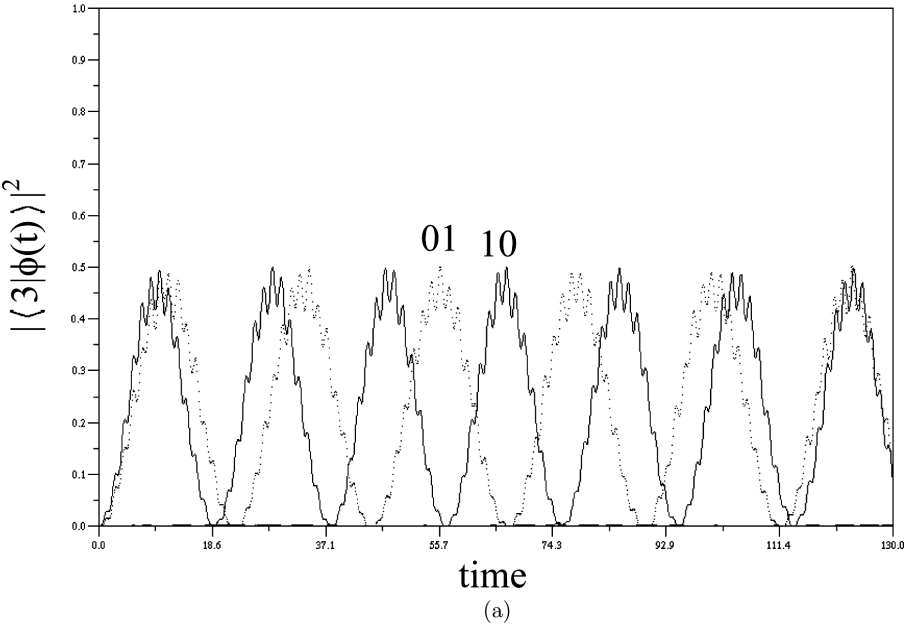

(a)

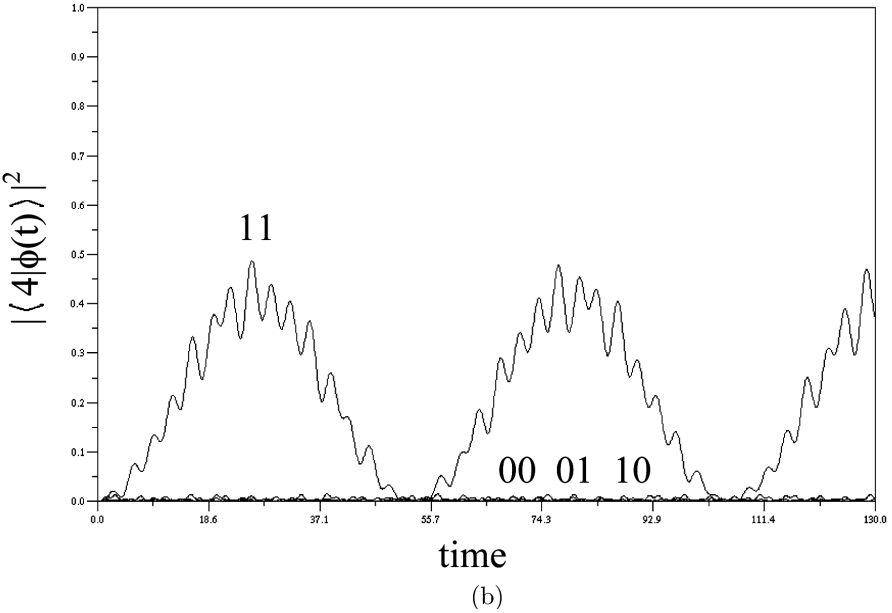

(b)

Fig. 4. Time evolution of the population of the XOR output level $|3\rangle$ and the AND output level $|4\rangle$ for the half-adder gate made of six levels and optimized using the "max" criterion. Figure (a) shows the XOR output with a large occupation only for the 10 and 01 inputs, and zero otherwise. Figure (b) displays the AND output with a large population only for the 11 input. The logic levels are defined according to the truth Table 4 (the time scale is $h/2e\pi$).

Table 4. Truth table of the half-adder Hamiltonian gate optimized with the "max" criterion leading to the H_{cal} Hamiltonian (8).

Logic input	α_1	α_2	XOR: max. of $\lvert\langle 3\lvert\phi(t)\rangle\rvert^2$	AND: max. of $\lvert\langle 4\lvert\phi(t)\rangle\rvert^2$
0 0	2	2	1.533×10^{-3}	6.48×10^{-3}
0 1	2	2/3	0.50791	1.55×10^{-2}
1 0	2/3	2	0.50791	9.98×10^{-3}
1 1	2/3	2/3	3.784×10^{-3}	0.5046

remaining on the internal levels supported by H_{cal} (e.g., the level $|4\rangle$ needed to readout the outcome of the AND gate). Recondensing the population only on the AND output of the gate will destroy the possibility of optimizing the XOR output. There is here a delicate balance to respect between finding an optimal solution such that the maximum population is reached on either the XOR or the AND output levels of the half-adder gate.

6. Conclusion

Compared to a quantum logic gate architecture, our new design takes benefit of the Heisenberg–Rabi oscillation of a single intramolecular electron transfer process. This opens the possibility to use, for example, a large part of the electronic degrees of freedom inside a single molecule, which are generally delocalized on the whole molecule for a conjugated molecule. Our design is also well adapted to high-conductance molecules because the square of the electron transfer rate is proportional to the electronic transparency of a molecular wire.[10] This rate is given by the frequency of the Heisenberg–Rabi oscillation of the electron transfer process through the molecule. Playing with oscillation frequency and not with population will open the way to drive a computation using the tunneling electrons of a tunnel junction. But we emphasize that, in such a design, the tunneling current will not carry information about the running computation. Inputs and ouputs will be taken from inside the molecule and not on the driving tunnel junction. Specific molecules are now under design to approach, in their monoelectronic structure, the optimized model Hamiltonians presented here. We want to integrate a logic function inside a single molecule without forcing the molecule to have the shape of an electrical circuit.

Acknowledgment

We thank the European IST project "Consortium for Hamiltonian Intramolecular Computing" (CHIC) for its financial support during this work.

References

1. F. Moresco, L. Gross, M. Alemani, K. H. Rieder, H. Tang, A. Gourdon and C. Joachim, *Phys. Rev. Lett.* **91**, 36601 (2003).

2. G. V. Nazin, X. H. Qiu and W. Ho, *Science* **302**, 77 (2003).
3. R. P. Feynman, *Optical News*, 11 February 1985.
4. C. Joachim, *Nanotechnology* **13**, R1 (2002).
5. C. Joachim, *J. Phys. A* **20**, L1149 (1987).
6. F. Moresco, G. Meyer, K. H. Rieder, H. Tang, A. Gourdon and C. Joachim, *Phys. Rev. Lett.* **86**, 674 (2001).
7. B. C. Stipe, M. A. Rezai and W. Ho, *Science* **279**, 1907 (1998).
8. J. Fiurasek, I. Duchemin, N. J. Cerf and C. Joachim, *Physica E* **24**, 161 (2004).
9. C. Joachim, *Chem. Phys.* **116**, 339 (1987).
10. C. Joachim and M. Ratner, *Nanotechnology* **15**, 1065 (2004).